$$C(hi\sigma\,,\ hi\sigma\,;\ \eta_1,\ \eta_2,\ \eta_3)=1,\quad i=1 \text{ or } 2 \tag{B11}$$

$$C(h1\sigma,\ h2\sigma;\ \eta_1,\ \eta_2,\ \eta_3)=\beta_\sigma[\tfrac{1}{2}n_\sigma(1-\tfrac{1}{2}n_\sigma)]^{-1}\,[1+(\lambda_\rho+\mu_\rho)\eta_2\eta_3+\lambda_\rho\mu_\rho\,\eta_1^2\,\eta_2^2\,\eta_3^2\,], \tag{B12}$$

$$C(h1\sigma, g1\sigma;\eta_1,\ \eta_2,\ \eta_3)=\alpha\beta_\sigma(\omega_\sigma+\nu_{123})\,[(\tfrac{1}{2}n_\sigma)(1-\tfrac{1}{2}n_\sigma)\,\omega_\sigma]^{-1}$$
$$\times[1+\chi_\sigma\,\eta_1+\lambda_\rho\eta_2+\mu_\rho\,\eta_3+(\lambda_\rho\mu_\rho+\mu_\rho\,\chi_\sigma+\chi_\sigma\lambda_\rho)\,\eta_1\eta_2\eta_3+\lambda_\rho\mu_\rho\chi_\sigma\eta_1^2\,\eta_2^2\,\eta_3^2\,]^2, \tag{B13}$$

$$C(h1\sigma\,,\ g2\sigma\,;\eta_1\,,\ \eta_2\,,\ \eta_3)=\alpha\beta_\sigma(\omega_\sigma+\nu_{123})\,[\tfrac{1}{2}n_\sigma(1-\tfrac{1}{2}n_\sigma)\,\omega_\sigma\,]^{-1}$$
$$\times\prod_{i,j}\{1+\lambda_\rho\,\eta_2+\mu_\rho(1+\lambda_\rho\,\eta_1^2\,\eta_i)\,\eta_j+[1+\lambda_\rho\,\eta_i\,\eta_j^2+\mu_\rho\,\eta_i\,\eta_j(1+\lambda_\rho\,\eta_1^2\,\eta_i\,\eta_j^2)]\chi_\sigma\,\eta_1\}. \tag{B14}$$

In (B14) $i=2$ and $j=3$, or $i=3$ and $j=2$. The other coefficients $C(h2\sigma,\ h1\sigma;\ \eta_1,\ \eta_2,\ \eta_3)$, $C(h2\sigma,\ g2\sigma;\ \eta_1,\ \eta_2,\ \eta_3)$, and $C(h2\sigma,\ g1\sigma,\ \eta_1,\ \eta_2,\ \eta_3)$ are obtained from (B12)–(B14) by exchanging 1 and 3, and 2 and 4 of the indices of ν. For strong correlation such that the triple and quadruple occupations are negligible, (B11)–(B14) reduce to (36)–(38).

---

*Parts of this work were reported in J. Appl. Phys. 42, 1420 (1971).

†Present address: Institute of Theoretical Physics, Fack, S-402 20, Göteborg 5, Sweden.

[1]J. C. Slater, Phys. Rev. 49, 537 (1936).

[2]E. P. Wohlfarth, Rev. Mod. Phys. 25, 211 (1953); J. C. Slater, *ibid.* 25, 199 (1953); C. Zener and R. R. Heikes, *ibid.* 25, 191 (1953).

[3]J. H. Van Vleck, Rev. Mod. Phys. 25, 220 (1953).

[4]H. Hurwitz, thesis (Harvard University, 1941) (unpublished); J. H. Van Vleck, Rev. Mod. Phys. 17, 42 (1945); Physica 15, 204 (1949).

[5]M. C. Gutzwiller, Phys. Rev. Letters 10, 159 (1963); Phys. Rev. 134, A923 (1964); 137, A1726 (1965), to be referred to as GIII.

[6]J. Hubbard, Proc. Roy. Soc. (London) A276, 238 (1963); 277, 238 (1964).

[7]J. Kanamori, Progr. Theoret. Phys. (Kyoto) 30, 275 (1963).

[8]W. F. Brinkman and T. M. Rice, Phys. Rev. B 2, 4302 (1970).

[9]N. F. Mott, Proc. Phys. Soc. (London) 62, 416 (1949); Phil. Mag. 6, 287 (1961); 40, 677 (1968).

[10]J. Hubbard, Proc. Roy. Soc. (London) A285, 542 (1965).

[11]Y. Nagaoka, Phys. Rev. 147, 392 (1966).

[12]E. Lieb and D. Mattis, Phys. Rev. 125, 164 (1962).

[13]See E. A. Guggenheim, *Mixtures* (Oxford U. P., New York, 1952), p. 38.

[14]Determinants are written in abbreviated form as

$$\left(f(x-y)\,\middle|\,\begin{matrix}X\\Y\end{matrix}\right)=\begin{vmatrix} f(x_1,\ y_1) & f(x_1,\ y_2) & \cdots & f(x_1,\ y_n)\\ f(x_2,\ y_1) & f(x_2,\ y_2) & \cdots & f(x_2,\ y_n)\\ \cdots & \cdots & \cdots & \cdots\\ f(x_n,\ y_1) & f(x_n,\ y_2) & \cdots & f(x_n,\ y_n)\end{vmatrix},$$

where X and Y are ordered sets and $x_i\in X$, $y_i\in Y$.

[15]See R. M. Thrall and L. Tornheim, *Vector Spaces and Matrices* (Wiley, New York, 1957), p. 127.

[16]For details, see M. C. Gutzwiller, Ref. 5, GIII, Sec. 2.

PHYSICAL REVIEW B VOLUME 4, NUMBER 11 1 DECEMBER 1971

Mössbauer Study of Hyperfine Magnetic Interactions in Fe-Ga Solid Solutions*

L. R. Newkirk and C. C. Tsuei

W. M. Keck Laboratory of Engineering Materials, California Institute of Technology, Pasadena, California 91109

(Received 15 March 1971)

Mössbauer spectra have been obtained for bcc Fe alloys containing up to 25-at.% Ga in solid solution. The spectra have been analyzed in a manner which permits the study of the effect of configuration on the hyperfine magnetic field and on the isomer shift with very few prior assumptions. Various assumptions commonly made in handling data of this type have been examined in detail and their validity tested. The details of 16 different configurations are presented along with an empirical formula to describe the hyperfine field as a function of configuration and concentration.

I. INTRODUCTION

The range and strength of the hyperfine magnetic interaction in nondilute solid solutions is of general interest in understanding the mechanism which causes these alloys to be ferromagnetic. Many of

the properties of this interaction have been determined for several alloy systems, including Fe-Ga, by Wertheim *et al.*[1] and others.[2–7] However, in view of the number of assumptions made in these studies without explicit justification, a detailed reexamination of one of these systems with a somewhat different type of data analysis is justified. The present analysis is intended to evaluate the validity of these assumptions as well as to provide new information about the nature of the hyperfine magnetic interaction. It is also shown that the application of this type of analysis to Mössbauer data with small statistical scatter yields more information than the data are usually thought to contain. The system Fe-Ga was chosen because it is possible to retain the bcc structure with as much as 35-at.% Ga in solid solution by quenching from the liquid state. This wide range of solid solubility and the partial ordering which occurs in the region of 25-at.% Ga allows the study of the effects of 16 different nearest-neighbor and next-nearest-neighbor configurations, thus making possible a more thorough examination of the characteristics of the hyperfine coupling.

II. EXPERIMENTAL PROCEDURES

Each alloy was prepared by placing the appropriate amount of Ga (99.99% pure) inside a hollowed Fe rod (99.99% pure) and sealing it in an evacuated quartz tube. The Ga was then allowed to diffuse into the Fe for 10 days at 800 °C, following which the diffused ingot was induction melted several times on a silver boat.[8] Weight losses were less than 0.1% of the ingot weight, so the nominal compositions were taken as the actual ones. Foils about 60 μm thick, prepared using the piston and anvil technique,[9] were mechanically polished to a thickness of ~35 μm. All Mössbauer measurements were performed at room temperature using a constant acceleration drive of the type described by Kankeleit.[10] The radioactive source, obtained from the New England Nuclear Corp., was 10 mCi of Co^{57} diffused in Pd. At ambient temperature this source produced a single line emission with a linewidth of ~0.30 mm/sec. Following the collection of data for each specimen, the spectrometer was calibrated using a 0.001-in. Fe calibration foil (also supplied by the New England Nuclear Corp.). The calibration data were fitted using peak splittings of 10.657, 6.167, and 1.677 mm/sec, as given in Ref. 11, thereby specifying the conversion from channels to mm/sec. This method of calibration results in reasonable agreement between the accepted value of isomer shift for Fe in Pd with respect to pure Fe [-0.185 ± 0.01 mm/sec (Ref. 12)] and the value of -0.177 ± 0.001 mm/sec obtained in this work. The x-ray diffraction measurements used to confirm crystal structure and previously reported lattice spacings were performed using a 114.6-mm Debye-Scherer powder camera and Fe filtered Co $K\alpha$ radiation.

III. DATA ANALYSIS AND EXPERIMENTAL RESULTS

The method used to fit the Mössbauer data is based on the assumption that the properties associated with a given Fe atom depend only on the configuration of nearest and next-nearest neighbors. Each such configuration is treated as a separate Fe site, having its own hyperfine field, isomer shift, and intensity, independent of values for other configurations. In this way no prior restrictions are placed on these parameters, and they may assume whatever values best fit the experimental data. An atom in the bcc structure has eight nearest neighbors, and six next-nearest neighbors, resulting in $9 \times 7 = 63$ possible combinations of neighbors in the first two shells (this assumes that only the number of Fe atoms in a shell is important, not their actual arrangement). The maximum number of sites actually used to fit any set of data was limited to 12, which, with the exception of the alloy $Fe_{80}Ga_{20}$, was sufficient to account for (92–97)% of the Fe atoms. The analysis for $Fe_{80}Ga_{20}$ included 85% of the Fe atoms with the remaining 15% spread over many sparsely populated sites. The actual fitting was done using an iterative least-squares procedure similar to that described by Bent *et al.*[13] and assigning the same linewidth for all peaks in a given spectrum. Since several alloys required more fitting parameters than could be conveniently varied simultaneously, the parameters were arranged into three groups. Group I contained all the isomer shifts and hyperfine fields, group II contained the site probabilities, and group III contained the background level, linewidth, and peak ratios (H_1/H_3 and H_2/H_3). The fitting was then accomplished by alternately varying groups (I + III) and (II + III) until covergence was achieved.

The Mössbauer data for alloys containing up to 25-at.% Ga are shown in Fig. 1 along with the curves fitted by the procedure outlined above. The numerical information obtained from each spectrum including the background level and the total area under the spectrum is presented in Tables I and II. Figure 2 shows the Mössbauer spectrum of the alloy $Fe_{75}Ga_{25}$, including the peaks of the individual components, in order to illustrate the technique of fitting. Figures 3 and 4 show the variation of hyperfine field and isomer shift with Ga concentration for the configurations $(n, m) = (0, 0)$, $(0, 1)$, $(1, 0)$, $(1, 1)$, and $(2, 0)$, where n and m are the number of Ga nearest and next-nearest neighbors, respectively. These particular configurations were chosen because they span the largest concentration range. Figure 5 illustrates the variation with Ga concentration of the linewidth

of the individual Lorentzian peaks.

IV. DISCUSSION

The methods most commonly used to analyze Mössbauer data associated with solid-solution alloys generally employ several or all of the following assumptions: (i) The relationship between hyperfine field and the number of solute atoms in a particular shell is linear. (ii) The effects of various shells of atoms are additive. (iii) The relationship between isomer shift and the number of solute atoms in a particular shell is linear. (iv) No quadrupole admixture exists. (v) The hyperfine field and isomer shift are entirely determined by the first and second shells of neighboring atoms. The only factor implicity assumed at the start of this analysis was the fifth assumption, and even this was tested in a manner described later.

In order to facilitate the examination of the first two assumptions it is helpful to consider the reduced hyperfine field rather than the actual measured hyperfine field. If the reduced field is expressed as

$$H_r(n, m) = \frac{H(n, m, c)}{H(0, 0, c)}, \tag{1}$$

where $H(n, m, c)$ is the hyperfine field at an Fe atom with n and m Ga neighbors in the first and second shells, respectively, and Ga concentration c, then the effect of configuration may be examined independently of the concentration dependence. Figure 6 shows the variation of the reduced field as Ga atoms replace Fe in the nearest-neighbor shell while retaining six Fe atoms in the second shell. It is clear from this figure that the first assumption above is not at all valid over a wide range of neighbor configurations, although the deviation from linearity is small for arrangements close to that of pure Fe. In order to determine whether the effects of various shells are additive, it is necessary to obtain an empirical formula to describe the variation of reduced hyperfine field with the number of Ga atoms in a particular shell. An expression of the form

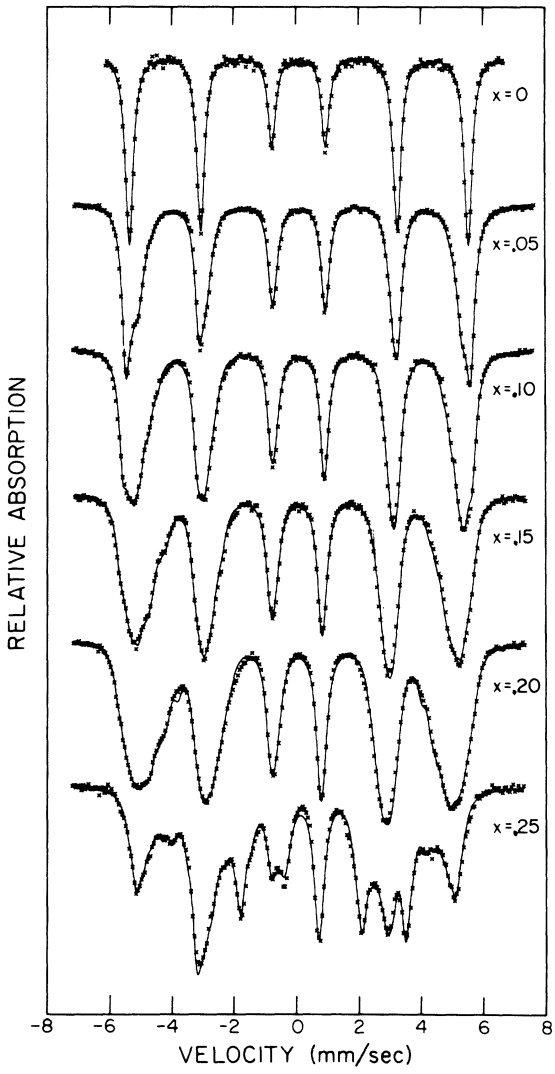

FIG. 1. Mössbauer spectra of the alloys $Fe_{1-x}Ga_x$. The solid line is the curve fitted by the method of least squares as described in the text.

$$H_1(n) = 1 + \alpha n + \beta n^2 , \tag{2}$$

where $H_1(n)$ is the reduced hyperfine field as a

TABLE I. The numerical values for background level (B), area, ratio of peak 1 to peak 3 (H_1/H_3), ratio of peak 2 to peak 3 (H_2/H_3), normalized chi squared (χ^2/N),[a] and the relative absorption of peak 1 for each alloy are shown below. Standard deviations are indicated by parenthesis.

Composition (at.% Ga)	B (counts)	Area (counts)	H_1/H_3	H_2/H_3	χ^2/N	Absorption (%)
0	165 595(44)	610 802	2.10(0.03)	1.95(0.03)	2.25	20.2
5	1 575 705(153)	483 771	2.64(0.02)	1.81(0.01)	7.19	8.9
10	3 112 213(246)	850 334	2.80(0.02)	1.98(0.01)	10.52	5.6
15	2 610 023(267)	707 786	2.81(0.02)	2.13(0.02)	7.17	4.5
20	4 883 698(380)	1 517 943	2.86(0.02)	2.10(0.01)	12.68	4.3
25	4 801 631(310)	973 043	2.61(0.02)	2.12(0.02)	6.54	2.2

[a] N is the number of degrees of freedom in each fit.

TABLE II. The numerical values of hyperfine field (HF), isomer shift (IS), and probability of occurrence (Intensity) for each configuration with n nearest and m next-nearest Ga neighbors are shown below for all the alloys studied. The standard deviations (shown in parenthesis) are calculated following inversion of the coefficient matrix during fitting.[a]

(n, m)	HF (kG)	IS (mm/sec)	Intensity
		Pure Fe	
(0, 0)	330 (0.1)	−0.177 (0.001)	1.000
		5-at.% Ga	
(0, 0)	334 (0.1)	−0.160 (0.001)	0.503 (0.004)
(1, 0)	313 (0.2)	−0.122 (0.002)	0.205 (0.005)
(0, 1)	322 (0.2)	−0.154 (0.003)	0.178 (0.004)
(1, 1)	302 (0.5)	−0.126 (0.005)	0.073 (0.004)
(2, 0)	288 (0.8)	−0.098 (0.008)	0.041 (0.003)
		10-at.% Ga	
(0, 0)	339 (0.1)	−0.139 (0.001)	0.237 (0.003)
(1, 0)	318 (0.2)	−0.112 (0.002)	0.188 (0.006)
(0, 1)	327 (0.2)	−0.135 (0.002)	0.182 (0.004)
(1, 1)	307 (0.5)	−0.096 (0.006)	0.086 (0.016)
(2, 0)	294 (1.6)	−0.077 (0.020)	0.104 (0.016)
(2, 1)	278 (0.5)	−0.061 (0.005)	0.053 (0.003)
(0, 2)	310 (1.4)	−0.098 (0.018)	0.119 (0.017)
(1, 2)	292 (3.3)	−0.074 (0.043)	0.031 (0.015)
		15-at.% Ga	
(1, 1)	307 (0.3)	−0.086 (0.003)	0.161 (0.006)
(1, 0)	320 (0.5)	−0.102 (0.005)	0.159 (0.006)
(0, 1)	330 (0.3)	−0.101 (0.003)	0.113 (0.005)
(0, 0)	341 (0.3)	−0.116 (0.003)	0.111 (0.003)
(2, 1)	283 (0.9)	−0.056 (0.003)	0.089 (0.007)
(2, 0)	296 (1.3)	−0.067 (0.013)	0.097 (0.009)
(1, 2)	290 (1.3)	−0.059 (0.019)	0.088 (0.011)
(0, 2)	315 (1.2)	−0.051 (0.016)	0.059 (0.007)
(2, 2)	270 (1.1)	−0.033 (0.008)	0.051 (0.006)
(3, 1)	254 (0.9)	−0.047 (0.010)	0.034 (0.004)
(3, 0)	262 (1.0)	−0.006 (0.012)	0.039 (0.006)
		20-at.% Ga	
(2, 1)	285 (0.2)	−0.039 (0.002)	0.127 (0.003)
(1, 1)	311 (0.5)	−0.066 (0.003)	0.121 (0.004)
(2, 0)	298 (0.4)	−0.105 (0.003)	0.095 (0.003)
(1, 2)	297 (0.3)	0.000 (0.002)	0.094 (0.003)
(0, 1)	334 (0.3)	−0.077 (0.003)	0.090 (0.003)
(2, 2)	272 (0.4)	−0.020 (0.003)	0.085 (0.003)
(1, 0)	324 (0.5)	−0.080 (0.006)	0.084 (0.007)
(3, 1)	255 (0.7)	+0.002 (0.004)	0.065 (0.003)
(3, 0)	263 (0.4)	−0.004 (0.005)	0.062 (0.004)
(3, 2)	236 (0.4)	+0.025 (0.003)	0.061 (0.002)
(0, 0)	345 (0.4)	−0.086 (0.004)	0.059 (0.002)
(0, 2)	319 (0.8)	−0.058 (0.010)	0.057 (0.007)
		25-at.% Ga	
(4, 0)	202 (0.2)	+0.103 (0.002)	0.294 (0.004)
(1, 1)	310 (0.7)	−0.063 (0.002)	0.187 (0.008)
(2, 0)	296 (1.0)	−0.057 (0.004)	0.106 (0.007)
(5, 0)	176 (0.5)	+0.155 (0.004)	0.087 (0.003)
(0, 5)	244 (0.6)	+0.020 (0.004)	0.081 (0.003)
(3, 0)	262 (0.8)	−0.006 (0.005)	0.069 (0.004)
(2, 1)	282 (1.2)	−0.038 (0.006)	0.065 (0.005)
(0, 6)	218 (0.8)	+0.065 (0.006)	0.064 (0.004)
(1, 0)	323 (1.1)	−0.069 (0.003)	0.047 (0.008)

[a]Described in Ref. 13.

function of n impurity nearest neighbors (with a pure Fe second shell), and α and β are constants, seems to be adequate to describe this variation. The constants α and β are determined by fitting the data with this function using the method of least squares. The solid line in Fig. 6 shows this fitted curve for the variation of $H_r(n, 0)$, while the dashed line indicates the variation assumed in Ref. 1 to treat this same system. If the variation of reduced field with second shell configuration (pure Fe first shell) $H_2(m)$ can be written in a similar form as

$$H_2(m) = 1 + \gamma m + \delta m^2, \tag{3}$$

then it is possible to test for additivity by attempting to fit all the data simultaneously to the function

$$H_r(n, m) = 1 + \alpha n + \beta n^2 + \gamma m + \delta m^2. \tag{4}$$

If a set of constants α, β, γ, and δ exists which fits the observed data, then this suggests that the effects are indeed additive. The determination of these parameters was also carried out by the least-squares method, and the resulting curves defined by Eq. (4) with $\alpha = 0.0495$, $\beta = 0.0106$, $\gamma = 0.0275$, and $\delta = 0.0057$, as well as the observed values, are shown in Fig. 7. The agreement of the data with the fitted curves seems close enough to imply that the second assumption is quite accurate.

The relationship between isomer shift and neighbor configuration is much more difficult to analyze. Figure 8 shows the variation of isomer shift with the number of Ga nearest neighbors (pure Fe second shell) at several Ga concentrations from 5 to 25 at.%. It is clear from this figure that the functional form of the variation of isomer shift with neighbor configuration is highly dependent on Ga concentration, and a linear approximation of the type used in Refs. 1 and 7 is valid only in the limit of low impurity concentration and for configurations close to pure Fe.

The absence of a quadrupole interaction in these alloys is most fortunate and deserves some attention. Despite the fact that the crystal structure is cubic, the local symmetry around an Fe atom with impurities in one of the first two shells, is, in general, not cubic, leading one to expect a quadrupole moment. Wertheim[1] has pointed out that the angle between the solute [111] and the direction of easy magnetization [100] is just right to cause the factor $(3\cos^2\theta - 1)$ to vanish, resulting in the quadrupole interaction having no influence on the location of the peaks. Unfortunately, this explanation applies only to the case of one solute atom located in the first shell. If one allows, for example, two impurity atoms in the first shell, then six of the seven possible configurations do not have a threefold or higher axis of rotational symmetry; hence, the usual formula[14] to describe the energy of each peak is invalid.

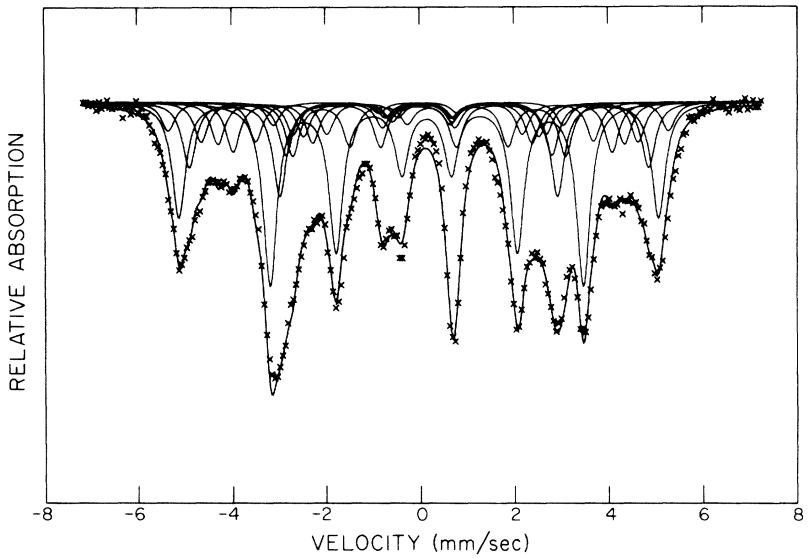

FIG. 2. Mössbauer spectrum of the alloy $Fe_{75}Ga_{25}$ including the individual peaks of the various components.

Cranshaw *et al.*[15,16] have shown by the use of single crystals that small anisotropic effects do exist in Fe-Si alloys which result in the broadening of certain components of the spectral lines. Although this does not necessarily imply that a quadrupole interaction exists in Fe-Ga alloys, the possibility must be carefully considered. In order to examine this possibility it is necessary to find an arrangement for which the formula considered above is valid, and to determine the direction in which the magnetic moments are aligned. In considering the second problem it is helpful to examine the intensity ratio of the second to the third peak in each spectrum, called H_2/H_3 in Table I. It is clear, from the formulas[14] defining the intensity dependence of these transitions on the angle between the incoming γ ray and the magnetic moment, that the ratio H_2/H_3 can vary from 0 to 4 depending on the alignment of the magnetic moment. For the particular case where the moments are arranged randomly with respect to the incoming γ ray (this also implies

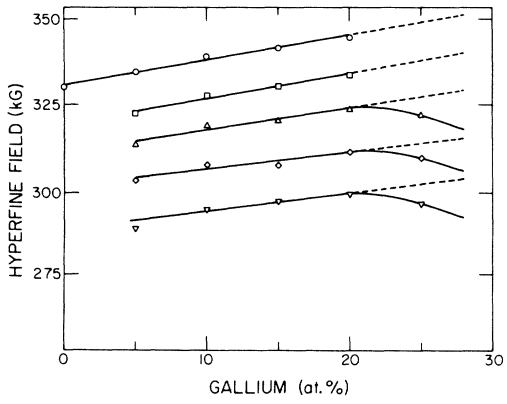

FIG. 3. Variation of hyperfine field with Ga concentration for the configurations $(n, m) = (0, 0)$(o); (0, 1) (□); (1, 0) (△); (1, 1) (◇); and (2, 0) (▽).

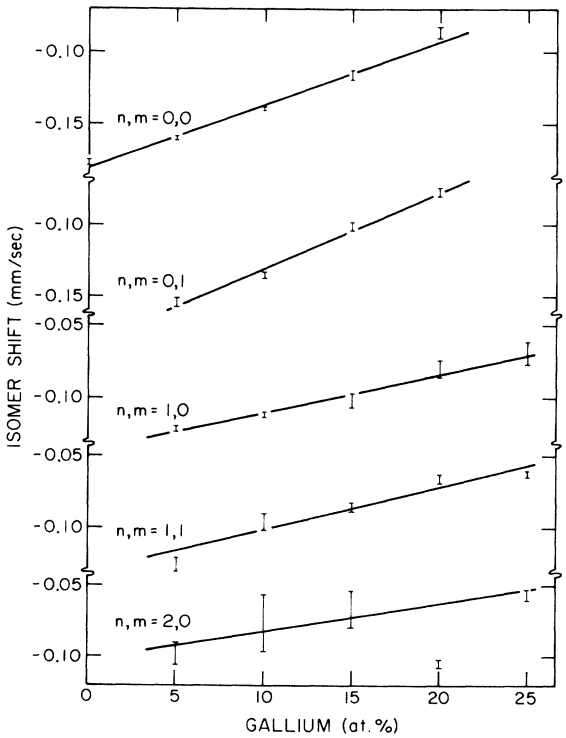

FIG. 4. Variation of isomer shift with Ga concentration for n and m Ga nearest and next-nearest neighbors, respectively.

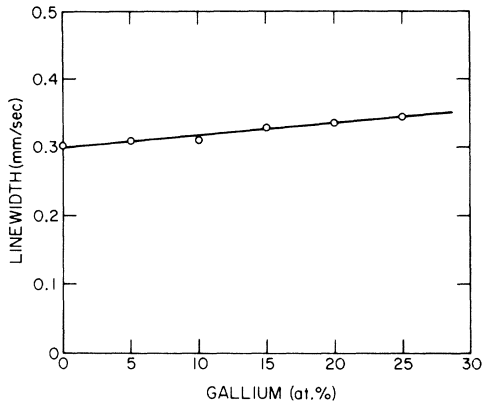

FIG. 5. Variation of the linewidth of the individual Lorentzian peaks with Ga concentration.

random arrangement with respect to the foil geometry) the spherical average of this dependence is such that $H_2/H_3 = 2$. The values of H_2/H_3 shown in Table I for the various specimens range from ~1.8 to ~2.1, indicating that for these samples the geometry of the foil has little or no influence on the direction of magnetization. This being the case, crystalline anistropy may be expected to dominate, resulting in the alignment of the magnetic moments along the direction of the easy magnetization [100] axis in bcc. It should be noted, in passing, that the intensity ratios of the first to the third peak, called H_1/H_3 in Table I, deviate somewhat from the theoretical value of 3. However, this is not related to the magnetization, since the angular dependence cancels out of this ratio, but rather it is caused by the finite thickness of the specimen.

The only configuration other than $n = 1$, $m = 0$, for which the formula for quadrupole admixture is valid, is the arrangement $n = 0$, $m = 1$. In this configuration, the electric field gradient tensor has a fourfold axis of rotational symmetry in the [100] direction which results in four arrangements with $\theta = \frac{1}{2}\pi$, one with $\theta = \pi$, and one with $\theta = 0$. Since we are interested in $(3\cos^2\theta - 1)$, both $\theta = 0$ and $\theta = \pi$ result in the same observed effect; consequently, the site $n = 0$, $m = 1$ is split into two sites whose intensity ratio is 2:1, with an observed quadrupole moment ratio of $-1:2$. The alloy $Fe_{90}Ga_{10}$, in which the site $n = 0$, $m = 1$ is one of the three most probable, was fitted allowing a quadrupole admixture of the type described above. The values for the quadrupole moments obtained from this fitting were less than 0.002 mm/sec, indicating that any quadrupole interaction was negligibly small. This would imply that the electric field gradient is not disturbed significantly by the presence of a Ga atom, indicating that the charge contrast must be fairly well screened. It is based on this test that the authors feel justified in ignoring any quadrupole admixture for all of the configurations studied.

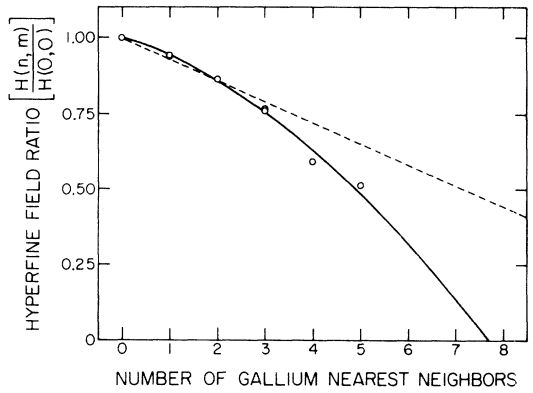

FIG. 6. Variation of reduced hyperfine field with nearest-neighbor configuration (pure Fe second shell). The solid curve is fitted according to Eq. (4).

A. Concentration Dependence of the Hyperfine Field

Wertheim *et al.*[1] observed as early as 1963 that the hyperfine field associated with an Fe atom surrounded by all Fe atoms (first and second shells) seems to increase with solute concentration regardless of the particular solute. As a consequence of this and other observations already discussed, the variation of hyperfine field with concentration and configuration is described in Ref. 1 as

$$H(n, m) = K_{Fe}(1 + kc)(1 + an + bm) , \qquad (5)$$

where c is proportional to concentration, k, a, and b are constants, and n and m are the numbers of nearest and next-nearest impurity neighbors. The

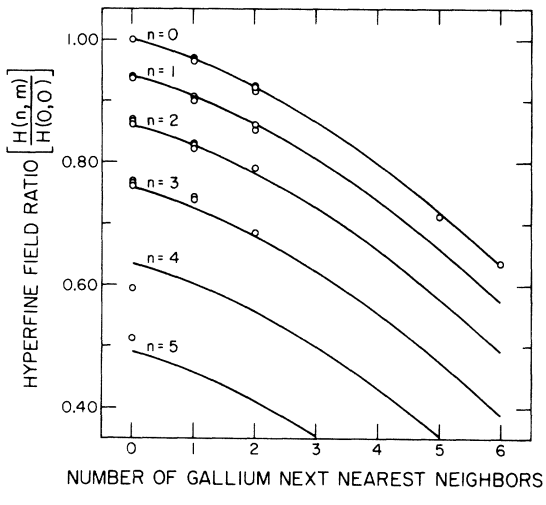

FIG. 7. Variation of reduced hyperfine field with configuration for n and m Ga nearest and next-nearest neighbors, respectively. The solid curves are fitted according to Eq. (4).

results of this study show that for concentrations less than 20-at.% Ga the hyperfine field for every statistically significant configuration increases with increasing Ga content. Using this information combined with that already presented regarding additivity of the effects of various shells, and the nonlinearity of adding impurity neighbors, an empirical expression similar to Eq. (5) may be written as

$$H(n, m) = H_{Fe} K(c)(1 + \alpha n + \beta n^2 + \gamma m + \delta m^2) , \quad (6)$$

where H_{Fe} is 330 kG, α, β, γ, and δ are the constants determined earlier, and c is Ga concentration. For alloys containing from 0 to 20-at. % Ga, examination of Fig. 4 shows that the concentration-dependent factor $K(c)$ can be represented as

$$K(c) = 1 + kc, \quad (7)$$

with $k = 0.24$. Above 20-at.% Ga this function is no longer linear, and the hyperfine field for a particular configuration decreases with increasing Ga content.

It is interesting to note that the shape of the curves in Fig. 4 is very similar to the data of Boyle and Hall[17] for Fe-Co alloys, in which the hyperfine field of Fe increases as d electrons are added, reaching a maximum with the addition of ~0.25 d electrons. In addition, the magnetization data of Aldred[18] show that the magnetic moment per Fe atom increases as Ga is added, and passes through a maximum at ~16-at.% Ga. However, as Wertheim has pointed out, and the present data confirm, the change in isomer shifts, both with configuration and concentration in Fe-Ga alloys, is much too small to be consistent with such a large electron transfer. This conclusion is based on the calculations of Walter *et al.*[19] for a nonionized Fe atom, which show that the addition of 0.25 d electrons would result in a change of 0.7 mm/sec in the isomer shift. Although other interpretations are possible if the atoms are allowed to be ionized, this is a very unlikely possibility, considering the absence of a quadrupole interaction. It seems more likely that the deviation from linearity, which occurs above 20-at.% Ga, is due to a sharp lowering of the Curie temperature caused by the partial BiF_3 ordering, similar to that which occurs in the Fe-Al system.[20]

B. Isomeric Shifts and Linewidth

Careful examination of Figs. 4 and 8 shows that while the variation of isomer shift with concentration seems to be almost linear, there is no obvious empirical formula which can characterize the variation with configuration. The general trend of the isomer shift to increase both with additional impurity neighbors and impurity concentration is consistent with the explanation in Ref. 1. As Ga is added to Fe the number of d electrons is increased slightly, resulting in more shielding of the 4s electrons from the nucleus. This causes a slight decrease in the electron density at the nucleus which results in an increase in the isomer shift.

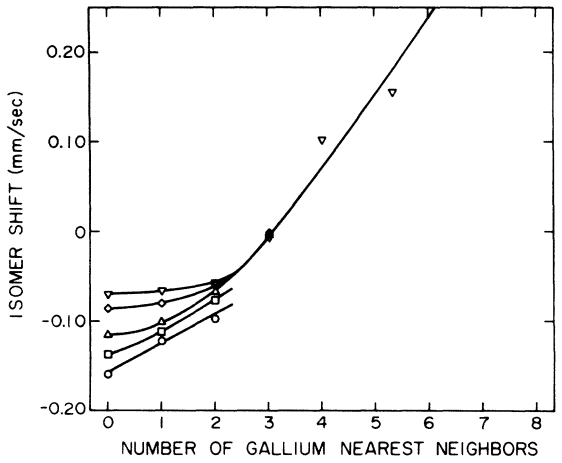

FIG. 8. Variation of isomer shift with nearest-neighbor configuration (pure Fe second shell) for 5-at.% Ga (o), 10-at.% Ga (□), 15-at.% Ga (△), 20-at.% Ga (◇), and 25-at.% Ga (▽).

In an analysis of the type presented here, the linewidth should be that of pure Fe and independent of concentration if the assumption made is exactly satisfied. Figure 5 shows that the linewidth increases slightly as Ga is added at the rate of 0.002 (mm/sec)/at.% Ga. This implies that the properties of a given Fe site are not entirely defined by the first two shells of neighbors, as was previously assumed. It is possible to determine whether the broadening is due to unresolved effects of the hyperfine magnetic interaction, the isomer shift, or both by determining whether the peaks are broadened equally or in an energy-dependent manner. The former is characteristic of a poorly defined isomer shift, and the latter is characteristic of a distribution of hyperfine fields. The data for the alloy $Fe_{85}Ga_{15}$ were fitted using a program option which allowed the linewidths of the peaks of a particular site to be determined by the formula

$$w = w_0 (1 + \alpha | E |) ,$$

where w is the width of peak of energy E, and w_0 and α are fitting parameters. The value of α determined by the least-squares procedure was ~0.001. For a maximum energy of 5 mm/sec, this implies a broadening of 0.0016 mm/sec, or only about 5% of the broadening actually observed. It may be concluded from this that the hyperfine field is well defined by the first two shells of neighbors, but the isomeric shift contains some unresolved effects of more distant atoms.

V. SUMMARY AND CONCLUSIONS

It has been shown for Fe-Ga alloys that a two-shell model employing superposition (additivity) of shells is quite adequate to study the hyperfine magnetic interaction. It seems likely that this type of model would also be applicable to iron alloys containing Al or Si. However, whether this model would adequately describe the properties of iron alloys containing elements from the first transition series is less clear and requires experimental data for verification. It has also been demonstrated that there is no reason for assuming a linear effect as impurity atoms are added to a particular shell. While the deviations are small for one or two impurity atoms, the error is quite severe when this information is extrapolated to other configurations. It seems reasonable to suppose that this type of nonlinear behavior is a general occurrence and that the use of a linear approximation is unacceptable for any solute.

The implications of the treatment of the quadrupole moment are also worth noting. Since it seems that shielding, rather than a specific relationship between crystallographic directions, leads to the disappearance of the quadrupole interaction in the Fe-Ga alloys, it is difficult to generalize the present results to other systems. It may well be that for other solutes near Fe in the Periodic Table, the screening is such that the electric field is not severely disturbed, but this is an uncertain conclusion until further evidence is obtained for other systems.

ACKNOWLEDGMENTS

The authors wish to express their appreciation for the advice of Professor Pol Duwez in conducting this study.

*Work supported by the U. S. Atomic Energy Commission.

[1]G. K. Wertheim, V. Jaccarino, J. H. Wernick, and D. N. E. Buchanan, Phys. Rev. Letters 12, 24 (1964).

[2]P. A. Flinn and S. L. Ruby, Phys. Rev. 124, 34 (1961).

[3]Mary Beth Stearns and Stephen S. Wilson, Phys. Rev. Letters 13, 313 (1964).

[4]Mary Beth Stearns, J. Appl. Phys. 36, 913 (1965).

[5]M. Rubinstein, G. H. Stauss, and M. B. Stearns, J. Appl. Phys. 37, 1334 (1966).

[6]Mary Beth Stearns, Phys. Rev. 147, 439 (1966).

[7]I. Vincze and L. Cser, Phys. Status Solidi 35, K25 (1969).

[8]H. F. Sterling and R. W. Warren, Metallurgia 67, 301 (1963).

[9]P. Pietrokowsky, J. Sci. Instr. 34, 445 (1962).

[10]E. Kankeleit, *Mössbauer Effect Methodology* (Plenum, New York, 1965), Vol. 1, p. 47.

[11]R. S. Preston, S. S. Hanna, and J. Heberle, Phys. Rev. 128, 2207 (1962).

[12]Arthur H. Muir, Jr., Ken J. Ando, and Helen M. Coogan, *Mössbauer Effect Data Index* 1958–1965 (Interscience, New York, 1966), p. 26.

[13]M. F. Bent, B. I. Persson, and D. G. Agresti, Comput. Phys. Commun. 1, 67 (1969).

[14]Gunther K. Wertheim, *Mössbauer Effect: Principles and Applications* (Academic, New York, 1964), p. 82.

[15]T. E. Cranshaw, C. E. Johnson, and M. S. Ridout, *Proceedings of the International Conference on Magnetism, Nottingham*, 1964 (The Institute of Physics and the Physical Society, London, 1965), p. 141.

[16]T. E. Cranshaw, C. E. Johnson, and M. S. Ridout, Phys. Letters 21, 481 (1966).

[17]A. J. F. Boyle and H. E. Hall, Rept. Progr. Phys. 25, 441 (1962).

[18]A. T. Aldred, J. Appl. Phys. 37, 1344 (1966).

[19]L. R. Walker, G. K. Wertheim, and V. Jaccarino, Phys. Rev. Letters 6, 98 (1961).

[20]Max Hansen, *Constitution of Binary Alloys* (McGraw-Hill, New York, 1958), p. 91.